Oxygen decreases in the eastern equatorial Pacific

Rena Czeschel[1], Lothar Stramma[1], and Gregory C. Johnson[2]

[1] IFM-GEOMAR, Leibniz-Institut für Meereswissenschaften, Düsternbrooker Weg 20, 24105 Kiel, Germany

[2]Pacific Marine Environmental Laboratory, NOAA, 7600 Sand Point Way NE, Seattle, WA 98115-6349, USA

14 October 2011

Corresponding author: Rena Czeschel, IFM-GEOMAR Leibniz-Institut für Meereswissenschaften, Düsternbrooker Weg 20, 24105 Kiel, Germany.

E-mail: rczeschel@ifm-geomar.de, Tel:+49-431-6004185; Fax:+49-431-6004102

Abstract

Observations indicate increasing oxygen minimum zones (OMZs) in the tropical Pacific over recent decades. Here we report on oxygen decreases within the eastern equatorial Pacific OMZ using data from repeat hydrographic sections at 110°W and 86°W, as well as from time series constructed from historical and profiling float oxygen data. In the section data, a general trend of decreasing oxygen is present below the surface layer. Furthermore, while velocity differences appear related to oxygen differences in some locations, especially the equatorial channel, they do not in others. Historical data are quite sparse for constructing oxygen time-series, but floats with oxygen sensors prove to be good tools to fill measurement gaps in later parts of these time series. In the future floats with oxygen sensors might play an important role in allowing construction of nearly continuous time-series in regions with sparse or infrequent ship-based hydrographic surveys. In the eastward flow region just south of the equator a time-series over the last 34 years reveals that oxygen decreases from 200–700 m at a rate between 0.5 and 0.9 μmol kg^{-1} yr^{-1}. Oscillations on shorter time scales (e.g., an El Niño signal in the upper 350 m) are superimposed upon this trend.

1. Introduction

Layers with particularly low oxygen concentrations, or oxygen minimum zones (OMZs), are located in the eastern tropical oceans at depths of 100–900 m [e.g. *Karstensen et al.,* 2008]. Century-long integrations of biogeochemical climate models under global warming conditions

predict an overall decline in oceanic dissolved oxygen concentration and expansion of the mid-depth OMZs [*Bopp et al.,* 2002; *Oschlies et al.*, 2008]. Predicted oxygen changes in the thermocline waters result largely from solubility changes in the upstream source waters, whereas changes in the deeper water mainly result from decreased interior advection and ongoing oxygen consumption by remineralization of sinking particulate organic matter [*Matear and Hirst,* 2003]. In the eastern South Pacific the OMZ is located off Peru, with its center being a stagnant area where floats with a parking depth of 400 m have remained for long periods [*Czeschel et al.,* 2011].

Eastward current bands in the eastern tropical Pacific [*Kessler,* 2006] could be important in resupplying oxygen to the OMZs [*Stramma et al.*, 2010a]. The most prominent eastward current with a subpycnocline expression is the Equatorial Undercurrent (EUC), which flows eastward along the equator across the entire Pacific [*Johnson et al.,* 2002]. Eastward surface-intensified currents include the weak South Equatorial Countercurrent (SECC), mainly observed in the western basin, and the North Equatorial Countercurrent (NECC), also prominent in the eastern basin (Figure 1). The Pacific subsurface countercurrents (SSCs, also known as Tsuchiya jets) are narrow eastward currents that bracket the equator just below the equatorial thermocline. The northern SCC (NSCC) and the southern SCC (SSCC) start around ±3° from the equator in the western Pacific, then gradually diverge and shoal to the east, with cores around ±6° from the equator and 150 m below the surface by 110°W [*Rowe et al.,* 2000]. At about ±2° from the equator from 500 to 1500-m depth weaker eastward current extrema exist [*Firing et al.*, 1998] – the North and South Intermediate Countercurrents (NICC, SICC). The North Equatorial Current (NEC) and the South Equatorial Current (SEC) are westward surface-intensifed currents. A

northern branch of the latter is often observed north of the equator. At mid-depth a westward North Equatorial Intermediate Current (NEIC) and a South Equatorial Intermediate Current (SEIC) centered around 500 m and 3° from the equator are observed [*Firing et al.,* 1998]. A westward Equatorial Intermediate Current (EIC) is found below the EUC preferentially in the western Pacific. Investigation of the supply paths of oxygen-rich water to the OMZs of the eastern North and South Pacific via zonal tropical currents demonstrated that eastward flow there were about 10–50 μmol kg^{-1} oxygen-richer than the westward current bands [*Stramma et al., 2010a*].

The Galapagos Islands at and south of the equator at 90–92°W are a topographic barrier for the EUC and for the westward flowing SEC [*Eden and Timmermann*, 2004] that lies within the eastern Pacific OMZ. Some locations of the equatorial Pacific are well sampled by Tropical Atmosphere Ocean (TAO) project cruises; however, we are not aware of a comprehensive observational dataset suitable for describing the structure and pathways of the EUC east of 95°W. *Karnauskas et al.* [2010] used the available data and model results to describe the interaction between the EUC and the Galapagos Islands but state that the nature of the EUC-like flow at ~85°W remains a challenging mystery.

Oxygen levels in the tropical Pacific OMZs appear to be decreasing, and the OMZ expanding. In 10°×10° areas of the tropical Pacific Ocean centered at the equator at 170°W and 110°W decreasing oxygen trends up to 0.2 μmol kg^{-1} yr^{-1} were observed over the last 50 years [*Stramma et al.,* 2008]. Smaller boxes between 3°N and 3°S at 170°W, 140°W, 110°W, and 95°W showed oxygen content decreasing as rapidly as -0.55 μmol kg^{-1} yr^{-1} for a 200-700 m layer over the last 30 years, with similar trends for a density layer spanning roughly these depths [*Stramma et al.,*

2010a]. A comparison of the two time periods 1960–1974 and 1990–2008 over 200–700 m showed a general decreasing oxygen trend for the equatorial and tropical Pacific [*Stramma et al.*, *2010b*]. Decreasing dissolved oxygen concentrations might have dramatic consequences for microbial and chemical cycling of nutrients and entire open ocean ecosystems. For example, shoaling of the tropical OMZ restricts the distribution of tropical pelagic fishes by compressing their habitat within the oxygenated surface layer [*Prince and Goodyear*, 2006].

2. Data

Historical quality-controlled hydrographic data from the HydroBase2 data set [*Curry*, 2008] available as of October 2008 are used for studying the oxygen distribution and its changes in the tropical Pacific. Data used are from the World Ocean Database 2001 [e.g., *Boyer et al*., 2006] and other programs, e.g., the World Ocean Circulation Experiment (WOCE). The data set is augmented with additional recently collected data sets in the eastern tropical Pacific [*Stramma et al.*, 2010b]. Along 110°W and 86°W (Figure 2) oxygen distributions from the WOCE period are compared with those from recent surveys to show the depth-dependant oxygen changes versus latitude across the equator. Finally data from five floats with oxygen sensors deployed in February 2009 along 86°W are used to extend time series of historical oxygen measurements.

WOCE section P18, along about 103°W south of 10°S and at 110°W north of 5°S was carried out on the NOAA Ship *Discoverer* from January–April 1994. Due to the diagonal course between 10°S and 5°S the section is used only north of 5°S. CTD and oxygen sample data were

collected and a lowered ADCP was attached to the CTD during the cruise. The cruise proceeded northward, crossing the equator on 13 April 1994. In December 2007 and January 2008 this section was repeated in southward direction with shipboard ADCP as well as a CTD with oxygen samples on the NOAA Ship *Ronald H. Brown*. Most of the stations used here were carried out in December 2007 with the 4°S station on 1 January, 2008, hence we will call this section the December 2007 section.

WOCE section P18 was occupied on the R/V *Knorr* from February–April 1993, with closely spaced full-depth stations across the equator from Southern Chile to Guatemala. This section runs along a nominal longitude of 88°W in the South Pacific but shifts to 85°50'W in the equatorial Pacific [*Tsuchiya and Talley*, 1998]. The shipboard ADCP sampling reached a maximum depth of 493 m. Lowered ADCP data were collected only north of 5°S and are used here to extend the vertical range of shipboard ADCP data. The cruise proceeded northward, crossing the equator on 30 March 1993. The northernmost station used here, at 2°N, was taken on 1 April, hence we call this section the March 1993 section. The CTD stations between 14°S and 2°N from this section were repeated during R/V *Meteor* cruise M77/4 in February 2009. The shipboard ADCP covered the upper ocean to 700-m depth.

Ten profiling floats with Aanderaa oxygen sensors were deployed from 2–11 February 2009 along the 85°50'W section, in pairs at 10°S, 8°S, 6°S, 4°S, and 2°S. One of each pair had a parking depth of 1000 dbar and the other 400 dbar, and all had 10-day surfacing intervals. The 400-dbar float deployed at 2°S had pressure sensor problems and its data are not used here. Five of the deployed floats (WMO 3901078, 79, 80, 81, and 84) crossed the boxes used here and their data are used in oxygen time series (Figure 2).

The Aanderaa oxygen sensors were calibrated for each sensor by comparing the first float profiles with ship-based CTD-oxygen casts co-located closely in time and space with the float deployments, as the floats started their mission with a deep profile, by a two-point calibration using the areas of maximum saturation at the near-surface and minimum saturation in the oxygen minimum layer. The calibrated dissolved oxygen (DO) concentration was then corrected for salinity and pressure effects using the float pressure and salinity readings (Aanderaa Manual, http://www.aadi.no), but using a higher pressure correction of 5.5% per 1000 dbar.

3. OMZ changes

3.1. The cross-equatorial sections

Long-term changes in the eastern equatorial Pacific oxygen distribution can be investigated by comparing oxygen and velocity data from the high-quality WOCE sections from the early 1990s to those from recent repeat surveys (Figure 3). On the 110°W section low oxygen concentrations are observed from 100–700-m depth and between 5°S and 10°N, with the strongest minimum (concentrations < 4 μmol kg^{-1}) at 500–700 m north of 8°N (Fig. 3a,b). Relatively high oxygen values of 20–40 μmol kg^{-1} are observed in the equatorial channel between 2°S and 2°N (Fig. 3a,b). This higher oxygen is clearly related to the EUC carrying oxygenated water eastward. The near-zero velocity at 400 m depth on the equator, below the EUC, may contribute to a local vertical oxygen minimum there (Fig. 3b).

Oxygen concentrations are generally lower for 100–400 m, and even down to 600 m north of the

146 equator, in late 2007 compared with 1994, independent of any velocity differences (Fig. 3c,
147 colors). The only exception is a region with an oxygen increase from 5–7°N. We investigate if
148 oxygen changes are related to velocity changes (Fig 3c, black contours). The velocity difference
149 at these latitudes shows increased eastward velocities of the NECC and the deeper NSCC,
150 consistent with these stronger currents carrying oxygen-richer waters into the region. Aside from
151 this band, the oxygen-poor layer extends further into the upper ocean in December 2007 (Fig. 3b)
152 leading to reduced oxygen values from 50–650 m in the north (Fig. 3c). In December 2007 the
153 eastward-flowing EUC was weaker and associated with lower oxygen values than in April 1994.
154 The westward-flowing SEC and the SEIC between 2°S and 4°S, which export oxygen-poor water
155 from the OMZ, are quite strong in 1994 compared with 2007 (Fig. 3a,b). While in the upper
156 ocean the weaker SEC in 2007 is associated with reduced oxygen values (Fig. 3c), the weaker
157 2007 SEIC is accompanied by enhanced oxygen values below 400 m.

158 At 85°50'W the analysis is limited to between 5°S and 2°N, where deep velocity measurements
159 exist for both cruises (Fig. 3d–f). In large parts of the upper 300 to 400 m the oxygen at
160 85°50'W decreases, while between ~300–400 and 700 m oxygen increases cover a larger cross-
161 section than decreases. The EUC was much stronger in March 1993 (Fig. 3d) than in February
162 2009 (Fig. 3e), and accordingly the equatorial upper ocean shows reduced oxygen with time (Fig.
163 3f), likely due to a reduced supply of oxygenated water. Below the EUC at 500 to 700-m depth
164 the westward flow at 0° to 1°N in March 1993 is probably a weak EIC. In 2009 a strong EIC is
165 observed between 1°S and 2°N and 200–400-m depth, perhaps causing a stronger westward
166 transport of oxygen-poor water from the OMZ (Fig. 3e) and a decrease in oxygen around the
167 equator at about 400-m depth (Fig. 3f). The northern part of the eastward flowing SSCC is well

168 visible south of 4.5°S in February 2009. As there was no SSCC in March 1993 the flow
169 difference for February 2009 is eastward and, at least below 300 m, the oxygen increase could be
170 related to the increased supply of oxygen-richer water in 2009. The 2009 section shows a
171 westward SEIC between 4.5°S and 3°S with a strong velocity core at about 500 m depth (Fig.
172 3e). The core of local minimum oxygen at 3.5°S in 500–600 m depth (Fig. 3f) is associated with
173 the stronger westward transport of deoxygenated water from OMZ in 2009. Similar to 110°W,
174 some oxygen changes appear related to velocity changes, especially in the equatorial channel.
175 However the anticipated accord between signs of zonal current and oxygen changes is only found
176 in slightly over 50% of the overall cross-sectional area considered for each section.

177

178 **3.2. Time series**

179 To improve interpretation of these snapshots we combined the oxygen data of the sections
180 discussed above with the quality-controlled historical data from the HydroBase2 dataset, recent
181 data from five profiling floats, and even ship-based CTD data at the float deployment positions,
182 to construct time series of the annual mean dissolved oxygen at various depths averaged yearly
183 within two near-equatorial boxes (A: 108–111°W, 5–2°S; B: 83–89°W, 5°S–equator). These
184 boxes were chosen to encompass a wide distribution of data from all decades. Both WOCE
185 sections cross these boxes and float profiles are in their midst.

186 Oxygen profiles with a vertical gap in sampling exceeding 100 m in the study depth range were
187 discarded. Over 90% of the oxygen data since 1929 were collected since 1976, so the latter is the
188 earliest year considered here. Oxygen data used appear to be of high quality and free from large

189 observational biases. For instance, time series for the upper 20-m depth are consistent with
190 expected saturated values, showing no trend for the last 34 years in both boxes. However, earlier
191 data do appear to show more year-to-year variability than more recent data (Fig. 4), perhaps
192 owing to larger random measurement noise. Seasonalities hardly affect the horizontal extent, core
193 thickness, or vertical depth range of the eastern tropical Pacific OMZ [*Paulmier and Ruiz-Pino*,
194 2009]. However, seasonality of the equatorial currents could influence the equatorial oxygen
195 distribution.

196 Linear trends and their 95% confidence interval [*Wunsch*, 1996] are computed using annual
197 averages of the profiles linearly interpolated to standard vertical levels. Degrees of freedom for
198 the confidence intervals are determined from integral time scales [*von Storch and Zwiers*, 1999].
199 All time series show a significant oxygen decrease for the last 34 years (Fig. 4), with trends
200 significantly different from zero at 95 % confidence (Table 1). The strongest (-0.94 ± 0.51 µmol
201 kg^{-1} yr^{-1}) trend is in the lower layer of the western part of the OMZ from 400–700-m depth (Fig.
202 4c). The time series for the layer between 400 – 700 m depth reveals an oxygen value far below
203 the trend line in 1994 (Fig. 4c), putting the slight increase of oxygen below 400-m depth between
204 the measurements along the 110°W section in 1994 and 2007 (Fig. 3c) into context.

205 In the eastern part of the OMZ (box B) the trend in oxygen decrease is strongest (-0.81 ± 0.44
206 µmol kg^{-1} yr^{-1}) in the upper OMZ layer between 200–400-m depth (Fig. 4e), consistent with the
207 overall decrease of oxygen in the upper 400 m shown along the 85°50'W sections between 1993
208 and 2009 (Fig. 3f). This pattern might be related to a stronger variability of the supply paths of
209 the upper OMZ: the EUC and SSCC. The annual mean in 1993 for the layer between 400 – 700
210 m (Fig. 4f) again shows an oxygen value below the overall trend line, again putting the slight

oxygen increase along the 85°50’ W sections between 1993 and 2009 below 400 m depth (Fig. 3f) into context.

4. Discussion

The variance explained by the linear oxygen trends is between 51% and 79% for the two boxes investigated (Table 1). Variability on shorter timescales or larger spatial scales may influence or alias the linear trends computed here. For instance, off California the observed oxygen changes over the last 57 years have not been monotonic, with earlier decreases reversing in the mid-1980s, bringing concentrations back up to levels measured in the late 1950s to early 1960s [*McClatchie et al.* 2010].

A model analysis [*Deutsch et al.*, 2011] suggests an association of the tropical Pacific OMZ strength with the Pacific Decadal Oscillation (PDO) index. In this model, decadal changes in respiration, driven by circulation changes, modulate the tropical Pacific OMZ so OMZ changes mirror, but in an amplified way, vertical excursions of the eastern thermocline associated with changes in the PDO index. These changes may be linked to observed decadal variability of the shallow Pacific meridional overturning circulation, with a decreasing trend in equatorial convergence from 1970 to the mid-1990s [*Zhang and McPhaden*, 2006] which should lead to a reduced equatorial circulation. This trend has reversed since the mid-1990s [*Schott et al.*, 2008]. The reversal could be related to a weakening in the trend of the eastern equatorial Pacific OMZ increase since the 1990s in most depths of the two boxes analyzed (Figure 4), however the trends

since 1993 at 110°W are not statistically significant and at 86°W there are only two years of data during this time period..

Complicating the interpretation further, on shorter time-scales El Niño events modify the thickness of the OMZ. At 4°S, 85°W, El Niño dynamics modulate mixed-layer depth, oxycline depth, and the vertical extend of the OMZ [*Fuenzalida* et al. 2009]. The upper 300 m of the OMZ, at this particular location, was replaced by oxygen-rich water during El Niño in December 1982 compared to December 1983 [*Fuenzalida* et al. 2009]. The WOCE survey of the 86°W section in March 1993 was made in a weak El Niño phase, while the February 2009 survey was occupied during weak La Niña conditions. A comparison of the data used here with the strong 1982 El Niño shows the strongest oxygen differences between about 50 to 150 m; however, the El Niño influence is visible down to about 350 m (Figure 5). Typical for El Niño conditions, in March 1993 the westward flow was larger and oxygen concentrations higher in the upper 200 m than in February 2009 (Figure 3d,e,f), while no clear El Niño signal can be assigned to the deeper part of the OMZ.

5. Summary

Our investigation shows overall reductions in oxygen content in the eastern equatorial Pacific OMZ over the last few decades with some variations superimposed. As the equatorial eastward currents carry slightly oxygen-richer water eastward towards the OMZ [*Stramma et al.* 2010a], some oxygen variability could be related to variations in velocity. A comparison of repeated

hydrographic sections at 110°W (1994 and 2007) and 85°50'W (1993 and 2009) shows that at some locations, especially near the equator, enhanced oxygen is related to stronger eastward flow; however, this result is not general, as countervailing regions are found. The decreasing trend seems to be in part a long-term OMZ change with some variability superimposed that could be related to decadal climate and circulation oscillations [*Deutsch et al.*, 2011; *Zhang and McPhaden*, 2006]. El Niño influences are also visible in upper 350 m of the 86°W section, but no clear influence is apparent below this depth.

Oxygen time series south of the equator covering the eastward current bands supplying oxygen-rich water to the OMZs at about 110°W and 86°W yielded trends of oxygen decrease for 200–700 m of -0.88 µmol kg^{-1} yr^{-1} and -0.51 µmol kg^{-1} yr^{-1}, respectively, over the last 34 years. Well-calibrated dissolved oxygen profiles from floats are useful in augmenting these time series in recent years. At 110°W the trend south of the equator is a little higher than a previously described decrease of -0.49 µmol kg^{-1} yr^{-1} [*Stramma et al.*, 2010a] centered on the equator. The continuous time series reveal that comparing only two sections may lead to erroneous conclusions, especially if El Niño events or decadal variations modify the upper ocean oxygen distributions during their occupation. The trends between the two section pairs for the layer 400 to 700 m depth within the range of the boxes used for the trend computations are positive at 110°W and negligible at 85°50'W (Fig. 4, dashed lines), while the long-term trend reveals a significant oxygen decrease. Trend computations for the western box since 1993 lead to a weakened negative trend for the 200-700 m layer, but the trend is not significant and hence it is not possible to prove a weakened oxygen decrease since the early 1990s with the present data set. Nevertheless comparing sections can lead to useful new results, as long as the differences

observed are interpreted with caution.

Acknowledgements. Financial support was received through the IFM-GEOMAR (R.C. and L.S.) and the NOAA Office of Ocean and Atmospheric Research (G.C.J.). This work is a contribution of the DFG-supported project SFB754 (www.sfb754.de) which is supported by the Deutsche Forschungsgemeinschaft. Findings and conclusions in this article are those of the authors and do not necessarily represent the views of the National Oceanic and Atmospheric Administration. PMEL publication 3759.

References

Bopp, L., C. Le Quere, M. Heimann, A. C. Manning, and P. Monfray (2002), Climate induced oceanic oxygen fluxes: Implications for the contemporary carbon budget, *Global Biogeochem. Cycles*, *16*, doi:10.1029/2001GB001445.

Boyer, T. P., J. I. Antonov, H. Garcia, D. R. Johnson, R. A. Locarnini, A. V. Mishonov, M. T. Pitcher, O. K. Baranova, and I. Smolyar (2006), World Ocean Database 2005, Chapter 1: Introduction, NOAA Atlas NESDIS 60, Ed. S. Levitus, U.S. Government Printing Office, Washington D.C., 182 pp., DVD.

Curry, R. (2008), http://www.whoi.edu/PO/hydrobase/.

Czeschel, R., L. Stramma, F. U. Schwarzkopf, B. S. Giese, A. Funk, and J. Karstensen (2011), Middepth circulation of the eastern tropical South Pacific and its link to the oxygen minimum zone, *J. Geophys. Res., 116*, C01015, doi:10.1029/2010JC006565.

Deutsch, C., H. Brix, T. Ito, H. Frenzel, and L. Thompson (2011), Climate-forced variability of ocean hypoxia, *Science., 333*, 336-339, doi:10.1126/science.1202422.

Eden, C., and A. Timmermann (2004), The influence of the Galapagos Islands on the tropical temperatures, currents and the generation of tropical instability waves, *Geophys. Res. Lett., 31*, L15308, doi:10.1029/2004GL020060.

Firing, E., S. E. Wijffels, and P. Hacker (1998), Equatorial subthermocline currents across the Pacific, *J. Geophys. Res., 103,* 21,413-21,423, doi:10.1029/98JC01944.

Fuenzalida, R., W. Schneider, J. Garces-Vargas, L. Bravo and C. Lange (2009), Vertical and horizontal extension of the oxygen minimum zone in the eastern South Pacific Ocean, *Deep-Sea Res. II, 56*, 992-1003.

Johnson, G. C., B. M. Sloyan, W. S. Kessler, and K. E. McTaggart (2002), Direct measurements of upper ocean currents and water properties across the tropical Pacific during the 1990's, *Prog. Oceanogr., 52*, 31-61, doi:10.1016/S0079-6611(02)00021-6.

Karnauskas, K. B., R. Murtugudde, and A. J. Busalacchi (2010), Observing the Galapagos-EUC interaction: Insights and challenges, *J. Phys. Oceanogr., 40*, 2768-2777.

Karstensen, J., L. Stramma, and M. Visbeck (2008), Oxygen minimum zones in the eastern tropical Atlantic and Pacific oceans, *Prog. Oceanogr., 77*, 331-350.

Kessler, W. S. (2006), The circulation of the eastern tropical Pacific: A review, *Prog. Oceanogr.*, *69*, 181-217.

Matear, R. J. and C. Hirst (2003), Long-term changes in dissolved oxygen concentrations in the ocean caused by protracted global warming, *Global Biogeochem. Cycles, 17,* 1125, doi:10.1029/2002GB001997.

McClatchie, S., R. Goericke, R. Cosgrove, G. Auad, and R. Vetter (2010), Oxygen in the Southern California Bight: Multidecadal trends and implications for demersal fisheries, *Geophys. Res. Lett., 37,* L19602, doi:10.1029/2010GL044497.

Oschlies, A., K. G. Schulz, U. Riebesell, and A. Schmittner (2008), Simulated 21st century's increase in oceanic suboxia by CO_2-enhanced biotic carbon export, *Global Biogeochem. Cycles, 22,* GB4008, doi:10.1029/2007GB003147.

Paulmier, A., and D. Ruiz-Pino (2009), Oxygen minimum zones (OMZs) in the modern ocean, *Prog. Oceanogr*., *80,* 113-128, doi:10.1016/j.pocean.2008.08.001.

Prince, E. D., and C. P. Goodyear (2006), Hypoxia-based habitat compression of tropical pelagic fishes, *Fish. Oceanogr., 15*, 451-464.

Rowe, G. D., E. Firing, and G. C. Johnson (2000), Pacific equatorial subsurface countercurrent velocity, transport, and potential vorticity, *J. Phys. Oceanogr., 30,* 1172-1187, doi:10.1175/1520-0485(2000)030<1172:PESCVT>2.0.CO;2.

Schott, F. A., L. Stramma, W. Wang, B. S. Giese and R. Zantopp (2008), Pacific subtropical cell variability in the SODA 2.0.2/3 assimilation, *Geophys. Res. Lett., 35*, L10607, doi:10.1029/2008GL033757.

Stramma, L., G. C. Johnson, J. Sprintall, and V. Mohrholz (2008), Expanding oxygen-minimum zones in the tropical oceans, *Science, 320,* 655-658.

335 Stramma, L., G. C. Johnson, E. Firing, and S. Schmidtko (2010a), Eastern Pacific oxygen
336 minimum zones: Supply paths and multidecadal changes, *J. Geophys. Res., 115*, C09011,
337 doi:10.1029/2009JC005976.
338 Stramma, L., S. Schmidtko, L. A. Levin, and G. C. Johnson (2010b), Ocean oxygen minima
339 expansions and their biological impacts, *Deep-Sea Res. I, 57*, 587-595.
340 Tsuchiya, M. and L. D. Talley (1998), A Pacific hydrographic section at 88°W: Water-property
341 distribution, *J. Geophys. Res., 103*, 12,899-12,918, doi:10.1029/97JC03415.
342 von Storch, H., and F. W. Zwiers (1999), The decorrelation time, in *Statistical analysis in*
343 *Climate Research*, chap. 17.1, pp. 371-374, doi:10.1017/CB09780511612336.018,
344 Cambridge Univ. Press, Cambridge, U.K.
345 Wunsch, C. (1996), Least squares, in *The ocean circulation inverse problem*, chap. 3.3, pp. 113-
346 119, doi:10.1017/CB09780511629570, Cambridge Univ. Press, Cambridge, U.K.
347 Zhang, D., and M. J. McPhaden (2006), Decadal variability of the shallow Pacific meridional
348 overturning circulation: Relation to tropical sea surface temperatures in observations and
349 climate change models, *Ocean Modelling, 15*, 250-273.
350
351
352
353
354
355
356

Figure captions

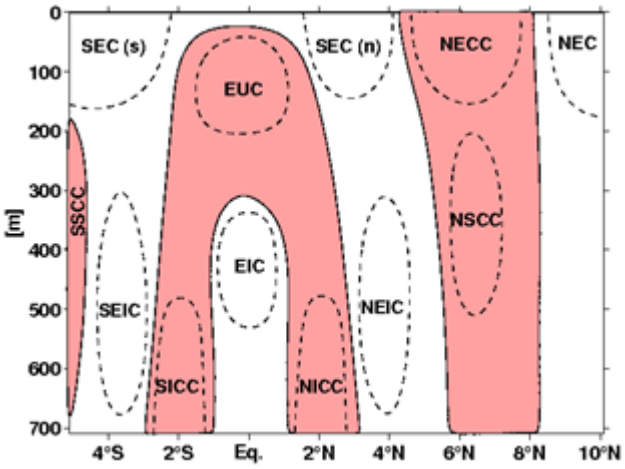

Figure 1. Schematic of zonal currents in the eastern equatorial Pacific, which might not be present or might be located at different locations in single surveys. For current names please refer to the text. Pink areas indicate eastward flow. Current cores are indicated by dashed lines.

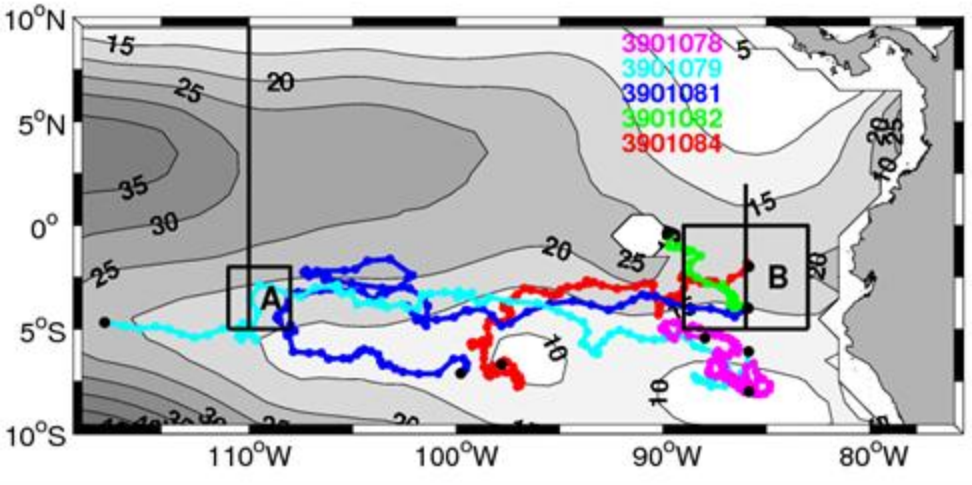

Figure 2. Mean climatological oxygen distribution (shaded contours, µmol/kg) at 400-m depth from WOA05 [Boyer et al., 2006] with WMO numbers and trajectories (in color) of the 5 floats which crossed the analyzed boxes A and B (black lines) between February 2009 and August 2011. The portions of the CTD sections used here along 110°W and 85°50'W are also indicated (solid lines).

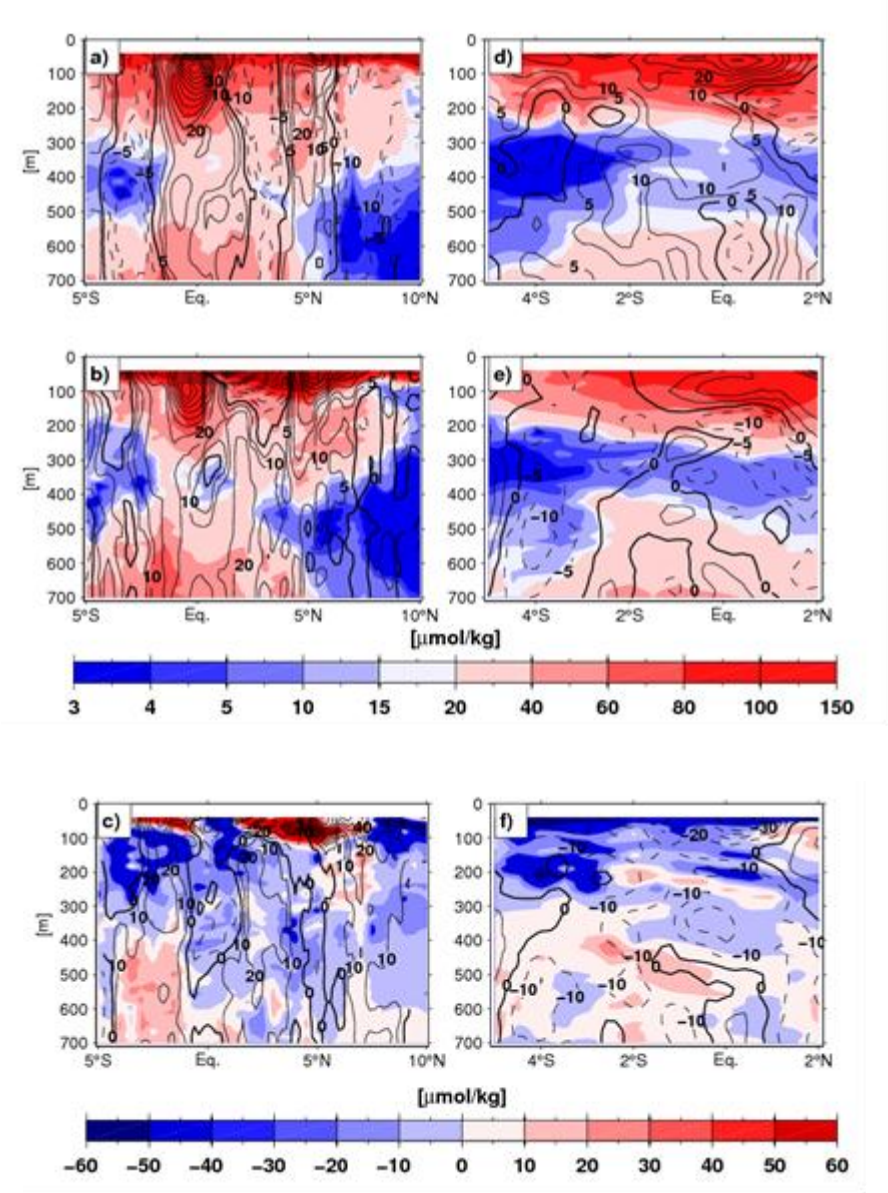

385

386

387 **Figure 3.** Dissolved oxygen distribution (color, µmol kg^{-1}) and ADCP-measured zonal velocity
388 distribution (black contours, cm s^{-1}, positive eastward) along 110°W a) in April 1994, b) in
389 December 2007–January 2008, and c) differences in oxygen (color, µmol kg^{-1}) and velocity
390 (black contours, cm s^{-1}, positive stronger eastward component in 2007) between the December
391 2007–January 2008 cruise and the April 1994 cruise. Dissolved oxygen distribution (color, µmol
392 kg^{-1}) and ADCP-measured zonal velocity distribution (black contours, cm s^{-1}, positive eastward)

along 85°50’W d) in March–April 1993, e) in February 2009, and f) differences in oxygen (color, μmol kg^{-1}) and velocity (black contours, cm s^{-1}, positive stronger eastward component in 2009) between the February 2009 cruise and the March–April 1993 cruise.

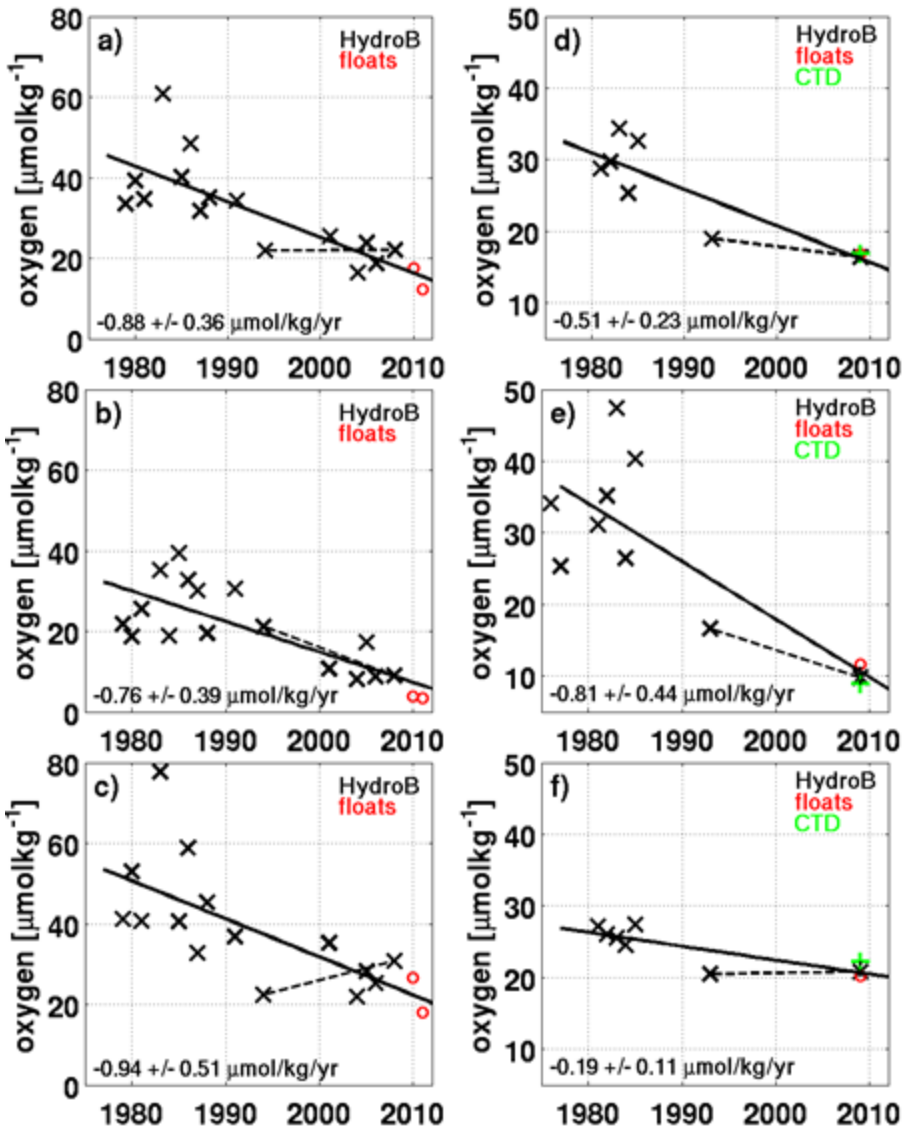

412

413 **Figure 4.** Time series of annual mean dissolved oxygen concentration (µmol kg^{-1}) from historical
414 data (black x's) since 1976, float data (red o's), and CTD data at float deployment locations
415 (green +'s) with linear fits (solid lines) for different depth levels. Analyzed boxes (see Fig. 2) are
416 bounded by 5–2°S, 108°–111°W (left panels) and 5°S–equator, 83–89°W (right panels). Depth
417 levels are 200–700 m (a, d), 200–400 m (b, e), and 400–700 m (c, f). Temporal oxygen trends
418 with 95% confidence intervals are included in each figure frame. The data of the two pairs of
419 sections (see Figure 3) are connected by dashed lines.

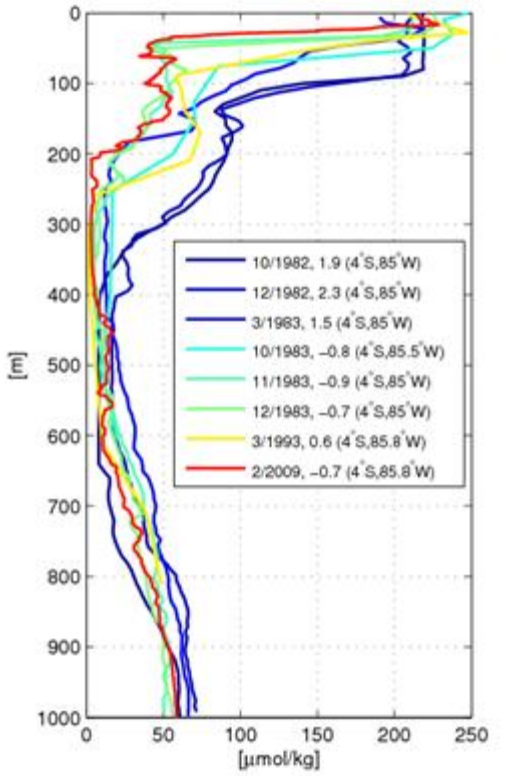

420

421 **Figure 5.** Dissolved oxygen profiles at about 4°S, 85°W during different El Niño periods (strong
422 are blue, weak are yellow) and La Niña phases (strong are blue-green and red are weak). Values
423 interpolated to section times from a 3-month running mean Oceanic Niño index (ONI.
424 [*http://ggweather.com/enso/oni.htm*]) are shown in the inset.

425

426

427

428

429

Area/depth layer	trend/confidence	variance	DOF
A: 200-700 m	-0.88+/-0.36	65 %	15
A: 200-400 m	-0.76+/-0.39	61 %	12
A: 400-700 m	-0.94+/-0.51	51 %	15
B: 200-700 m	-0.51+/-0.23	79 %	7
B: 200-400 m	-0.81+/-0.44	66 %	9
B: 400-700 m	-0.19+/-0.11	65 %	7

Table 1. Temporal oxygen trends (μmol kg^{-1} yr^{-1}) and their 95% confidence intervals from linear fits for boxes A (5–2°S, 108–111°W) and B (5°S–equator, 83–89°W) over three depth layers (Figure 4) with percentages of the total variance accounted for by those trends and the degrees of freedom (DOF).